The Effect of Heat Treatment on Microfissuring in Alloy 718

Changes in microfissuring susceptibility during heat treatment were found to correlate with movement of impurities to and from the grain boundaries

BY R. G. THOMPSON, J. R. DOBBS AND D. E. MAYO

ABSTRACT. The weldability of nickel base Alloy 718 has been shown to respond favorably to some heat treatments but unfavorably to others. Heat treatments common to this alloy, such as homogenization, solution anneal, and age hardening, have all been shown to have a measurable effect on the magnitude of heat-affected zone (HAZ) microfissuring. Such results have been reported consistently over the 20 years since the alloy was developed, even though the alloy's chemistry and microstructure have gradually been refined.

The purpose of the present program was to study the effect of heat treatment on HAZ microfissuring susceptibility. The study made the initial assumption that favorable or unfavorable weldability changes occurred during heat treatment, due to microstructural changes which also occurred during heat treatment. This hypothesis was tested by correlating the rate of change in HAZ microfissuring with the rate of change in microstructure during various heat treatments.

The results of the study showed that typical precipitation and hardening which occur during heat treatment do not correlate with changes in weldability. The changes in weldability during heat treatment were found to correlate better with the movement of impurities to and from the grain boundaries. These observations resulted in the proposal of a theory for microfissuring susceptibility based on intergranular impurity segregation during heat treatment.

Based on a paper sponsored by the WRC High Alloys Committee and presented at the 65th Annual AWS Convention, held April 9–13, 1984, in Dallas, Tex.

R. G. THOMPSON, J. R. DOBBS and D. E. MAYO are with the Department of Materials Engineering, University of Alabama at Birmingham (UAB).

Introduction

Alloy 718 has received widespread acceptance as one of the most easily welded metals for high temperature application. However, along with this reputation for good weldability has come a notoriety for microfissuring—the formation of intergranular cracks in the base metal heat-affected zone. Although it is not possible to determine if a given production weld will microfissure, it is possible to determine the relative microfissuring susceptibility of a metal in a given process state. The hot ductility test and Varestraint test are both suited for this task and their use has been reviewed previously (Refs. 1, 2).

The inherent microfissuring susceptibility of a metal has been shown to be a function of many metallurgical variables. These include heat-to-heat chemistry differences (Ref. 3), process condition (cast, wrought or forged) (Ref. 3), grain size (Ref. 4), and heat treatment (Refs. 5, 6). At present, no single mechanism or combination of mechanisms has been put forth which explains how these metallurgical variables interact to control a metal's microfissuring susceptibility. There is, however, a growing understanding of individual aspects of the microfissuring mechanism. For example, it is now known that increasing grain size, independent of other variables, causes increasing microfissuring susceptibility (Ref. 4). Thus, microfissuring has some functional dependence on a grain size variable, such as grain boundary surface area.

There continue to be more questions about the mechanism of microfissuring than answers. One question that has remained unanswered is why heat treatment has a strong effect on microfissuring susceptibility. It has been shown in several investigations that solution annealing reduces microfissuring susceptibility, while age hardening increases it (Refs. 3, 5, 6). Vincent (Ref. 7) suggested that $Ni_3Nb(\delta)$ precipitation during solution annealing increased microfissuring resistance. Although Duvall and Owczarski (Ref. 5) observed the difference in microfissuring susceptibility between the solution annealed and age hardened conditions, they did not speculate on the cause.

Thompson and Genculu (Ref. 6) also observed the beneficial effect of solution annealing and the detrimental effect of age hardening on microfissuring. They, like Duvall and Owczarski (Ref. 5), studied wrought alloy and found that microfissuring was initiated by the constitutional liquation of niobium-rich M(C,N) particles. Intergranular liquid produced by this reaction was found in both the solution annealed and age hardened conditions. Thompson and Genculu (Ref. 6) suggested that the microfissure-related difference in these heat treatments was the manner in which the intergranular liquid distribution was controlled by intergranular chemistry. This chemistry would be controlled by heat treatment.

The present paper investigates the differences between heat treatments relative to microfissuring susceptibility. The experimental techniques were specifically designed to eliminate the variables of grain size and heat-to-heat chemistry differences which often complicate interpretation of results. The results from this study are discussed in terms of the rate of change in microfissuring susceptibility during heat treatment. These microfissuring changes are correlated with the kinet-

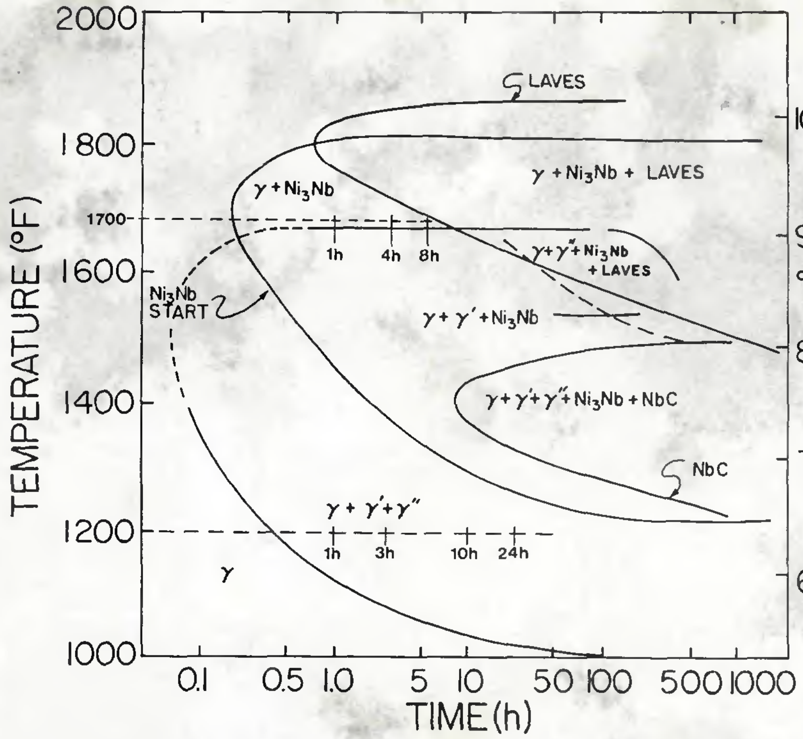

Fig. 1 — Transformation diagram for Inconel 718 showing heat treatment schedule

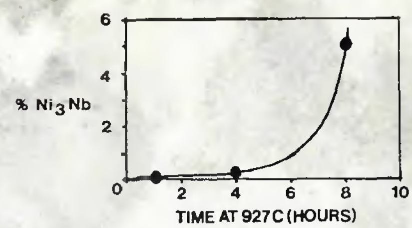

Fig. 2 — Rate of $Ni_3Nb(\delta)$ precipitation during solution annealing at 927°C (1700°F)

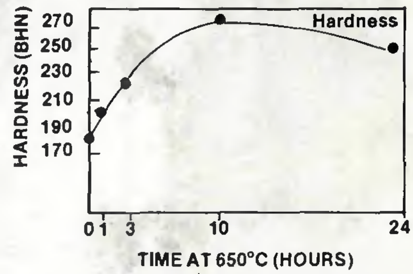

Fig. 3 — The rate of hardening during aging at 650°C. Grain size 60 μm

ics of phase changes and impurity segregation during heat treatment. This work is continuing with Auger spectroscopy studies on specially prepared alloy chemistries of 718.

Table 1—Chemical Analysis

C	0.04	Cr	18.35
Mn	0.10	Al	0.60
Fe	18.95	Ti	1.00
S	0.003	Co	0.10
Si	0.16	Mo	2.98
Cu	0.08	Nb + Ta	5.22
Ni	52.42		

Table 2—Heat Treatment

High-Temperature Anneal	
30μ grain size	30 s at 2130°F
60μ grain size	5 min at 2130°F
200μ grain size	24 h at 2130°F
Solution Anneal — high-temperature anneal plus one of the following:	
	1 h at 1700°F
	4 h at 1700°F
	8 h at 1700°F
Age Hardening — high-temperature anneal plus one of the following:	
	1 h at 1200°F
	3 h at 1200°F
	10 h at 1200°F
	24 h at 1200°F

Experimental Procedure and Results

Previous experience with wrought Alloy 718 had shown that solution annealing (approximately 950°C/1742°F) reduced microfissuring, while age hardening increased it. The experimental plan was developed to study the kinetics of the change in microfissuring susceptibility during these heat treatments. The experimental plan was further designed to investigate the effect of two microstructure changes which occur during these heat treatments, namely, $Ni_3Nb(\delta)$ precipitation during solution annealing and $\gamma' + \gamma''$ precipitation during age hardening. The TTT diagram shown in Fig. 1 for Alloy 718 was used to select heat treatments which would produce microstructures of interest.

All material was taken from the same ⅛-in. (3.2-mm) thick plate whose composition is given in Table 1. Specimens were initially given a high temperature anneal at 1165°C (2130°F), followed by quenching. This solutioned all phases except for the higher temperature carbides. A solution annealing treatment at 927°C (1700°F) was chosen to precipitate $Ni_3Nb(\delta)$, while avoiding either Laves or $\gamma' + \gamma''$ precipitation. This is shown in Fig. 1 where the heat treatment times at 927°C all fall in the γ + $Ni_3Nb(\delta)$ phase field. It was planned to investigate microfissuring susceptibility as a function of $Ni_3Nb(\delta)$ precipitation kinetics during solution annealing. Thus, annealing times of 1, 4 and 8 h were used to precipitate increasing volume fractions of $Ni_3Nb(\delta)$.

Table 3—Varestraint Test Parameters

Welding current, A	65
Welding voltage, V	12.5
Arc on time, s	10
Argon shielding, cfh	30
Electrode to work distance[a] mm (in.)	6.2 (0.245)

[a] 2% Thoria W electrode, 1/16-in. diameter, 60-deg included angle.

An unusual deviation from standard heat treating practice was used to produce the age hardened condition. The 718 alloy was aged at 650°C (1200°F) without first receiving a solution anneal. It can be seen from Fig. 1 that heat treating at 650°C falls in the $\gamma + \gamma' + \gamma''$ region of the TTT curve. Such a procedure should allow microfissuring susceptibility to be studied as a function of $\gamma' + \gamma''$ precipitation. By avoiding the solution anneal treatment it was hoped that precipitation of auxiliary phases such as Laves and $Ni_3Nb(\delta)$ would also be avoided. Table 2 summarizes the heat treatments used in this study.

The solution annealing treatment produced $Ni_3Nb(\delta)$ as expected — Fig. 1. The rate of $Ni_3Nb(\delta)$ precipitation is given in Fig. 2 for several grain sizes. (The method of producing this grain size range was discussed in an earlier publication (Ref. 4).) It is interesting to note that the larger grain sizes had longer annealing time at 1165°C (2130°F) and thus better alloy homogenization. This led to longer nucleation and growth time for $Ni_3Nb(\delta)$ precipitation in the metal with larger grain size. This in turn points out some of the limitations of using a "standard" TTT diagram, such as Fig. 1. It is quite obvious that the transformation kinetics are dependent on the degree of Nb homogenization in the metal.

The rate of $\gamma' + \gamma''$ precipitation was monitored using hardness tests and the rate of age hardening at 650°C is shown in Fig. 3. Typical microstructures of the solution annealed metal are shown in Fig. 4 and of the age hardened metal in Fig. 5.

Specimens heat treated as described in Table 2 were tested for their microfissuring susceptibility, using the spot Varestraint test. The operating characteristics of our equipment were discussed in an earlier paper (Ref. 4). Varestraint test variables are given in Table 3 and specimen preparation techniques were detailed in a previous publication (Ref. 4). All Varestraint tests were run using 1% augmented strain. The results of the Varestraint tests are shown in Figs. 6 and 7, with test data in Table 4.

Discussion

It is now well known that several wrought superalloys suffer heat-affected zone microfissuring due to the constitutional liquation of carbides, as described by Owczarski, Duvall and Sullivan (Ref. 8). Waspaloy (Ref. 8), Udimet 700 (Ref. 8), Hastelloy X (Refs. 5, 9), and Alloy 718 (Refs. 5, 6) have all been shown to exhibit such behavior. Alloy 718 has also been shown to be more susceptible to microfissuring in the age hardened condition than in the solution annealed condition (Refs. 5, 6). This is difficult to understand since both suffer constitutional liquation from niobium-rich carbonitrides (Ref. 6). The present study was undertaken to define the mechanism through which heat treatment affects microfissuring. If this mechanism were known, then it might be possible to accentuate the solution annealing effect or minimize the age hardening effect to improve the weldability of Alloy 718.

Results from this and other studies (Refs. 3, 5, 6) indicate that processing steps such as hot working, annealing and homogenization establish some baseline microfissuring susceptibility in Alloy 718. Solution annealing around 950°C (1750°F) has been shown to reduce this baseline microfissuring susceptibility. The microfissuring susceptibility is increased again if the solution annealed metal is then age hardened prior to welding. In order to study the solution anneal and age hardening heat treatments independently of each other, a nonconventional heat treatment scheme was employed, as shown in Table 5. Note that in Experiment II the age hardening is performed without first solution annealing the metal. The purpose of this procedure was to eliminate the $Ni_3Nb(\delta)$ precipitation characteristic of the solution anneal treatment. This would allow us to study the effect of hardness and $\gamma' + \gamma''$ precipitation on microfissuring susceptibility during age hardening independent of $Ni_3Nb(\delta)$. It was seen that $Ni_3Nb(\delta)$ precipitation did occur during age hardening in the 200 μm grain size samples, even though this would not have been predicted by Fig. 1.

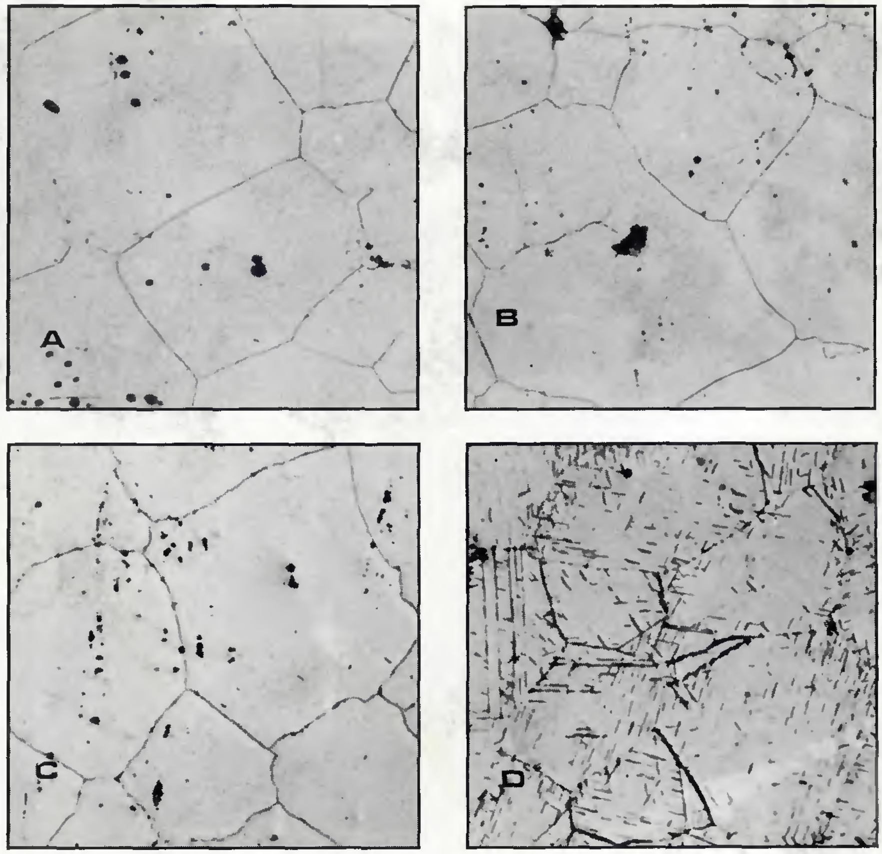

Fig. 4 — Typical microstructures of solution annealed Alloy 718. A — 0 h at 927°C; B — 1 h at 927°C; C — 4 h at 927°C; D — 8 h at 927°C. Grain size 200 μm

Table 4—Varestraint Test Data

Solution Annealed

Specimen Number	Grain Size (μm)	Time at 927° C (h)	Total Crack Length (μm)	Total Crack Number
31	30	0	13454	27
54	30	1	11403	26
93	60	0	16341	29
8	60	0	16047	36
39	60	1	15065	30
50	60	4	13041	22
49	60	8	11850	17
22	200	0	26415	37
29	200	0	22776	36
69	200	1	17669	26
85	200	4	16848	24
83	200	8	14813	20

Age Hardened

Specimen Number	Grain Size (μm)	Time at 650° C (h)	Hardness (BHN)	Total Crack Length (μm)	Total Crack Number
93	60	0	168	16341	29
8	60	0	—	16047	36
92	60	1	187	17088	25
88	60	3	217	17444	25
47	60	10	271	17903	26
89	60	25	238	18052	28

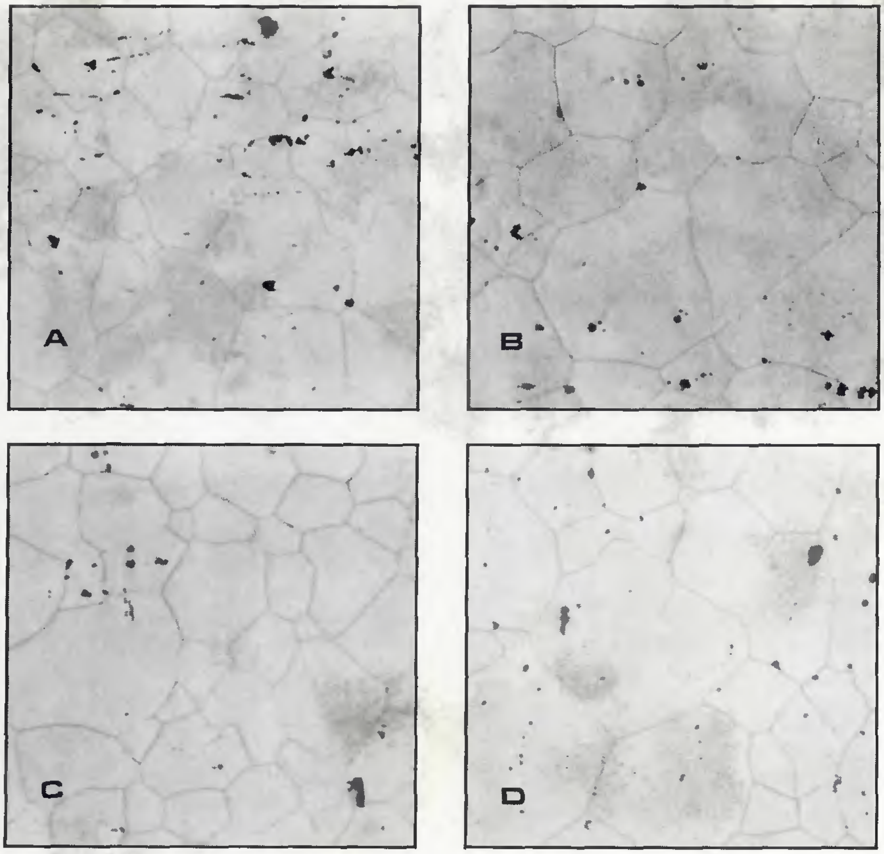

Fig. 5 — Typical microstructures of age hardened Alloy 718. A — 0 h at 650°C; B — 1 h at 650°C; C — 10 h at 650°C; D — 25 h at 650°C. Grain size 60 μm

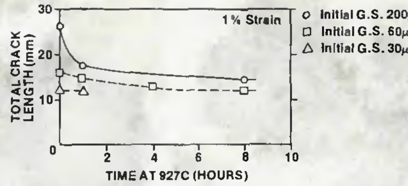

Fig. 6 — The change in microfissuring susceptibility during solution annealing at 927°C (typical scatter in the spot Varestraint test was 16% ± 4%)

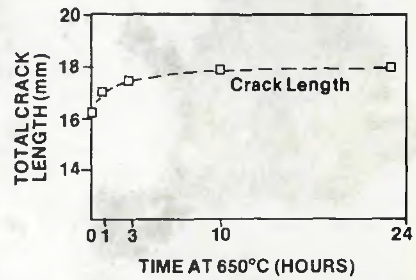

Fig. 7 — The change in microfissuring susceptibility during aging at 650°C. Grain size 60 μm

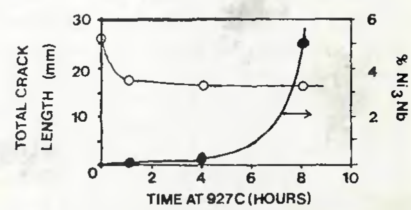

Fig. 8 — A comparison of the change in microfissuring susceptibility with the precipitation rate of $Ni_3Nb(\delta)$ during solution annealing

This precipitation occurred late in the heat treatment and was not believed to affect the experimental plan.

Experiment I was designed to evaluate the role $Ni_3Nb(\delta)$ precipitation on microfissuring susceptibility. Large grain size (or long homogenization treatment) metal gave larger reductions in microfissuring after the solution anneal treatment than metal of smaller grain size, as seen in Fig. 6. To determine if the decrease in microfissuring susceptibility was related to $Ni_3Nb(\delta)$ precipitation, the kinetics of these two processes were compared — Fig. 8. It was seen from this comparison that the $Ni_3Nb(\delta)$ precipitation was very sluggish and did not begin until after the change in microfissuring susceptibility was almost complete. Note also that when $Ni_3Nb(\delta)$ precipitation did begin, it had no effect on microfissuring susceptibility. It was concluded from these results that the change in microfissuring susceptibility during solution annealing was not due to the $Ni_3Nb(\delta)$ precipitation process. It must instead be related to some other process which occurred during solution annealing.

Experiment II was designed to determine if $\gamma' + \gamma''$ precipitation or an increase in hardness was responsible for the increase in microfissuring susceptibility during age hardening. It was assumed that the kinetics of the hardness change during aging were representative of the $\gamma' + \gamma''$ precipitation kinetics. As with the solution annealed metal, a comparison was made between the kinetics of microfissuring increase during age hardening and the rate of change in hardening. This comparison is shown in Fig. 9.

It was seen from this comparison that the increase in microfissuring occurred prior to appreciable hardening. Furthermore, the hardness continued to increase, while the microfissuring showed no change. Based on the assumption that hardness reflected $\gamma' + \gamma''$ precipitation, it was concluded that neither matrix hardness nor $\gamma' + \gamma''$ precipitation controlled the change in microfissuring during age hardening.

The original question of this paper was: Why does microfissuring susceptibility change during heat treatment? The experimental design prevented several factors which normally influence microfissuring susceptibility from affecting microfissuring results in the present study. These were heat-to-heat chemistry dif-

Table 5—Experimental Plan

Typical Treatment	Prior Processing	+	Solution Anneal 1750° F	+	Age Hardening 1400° F + 1200° F
Microstructure changes	Process dependent		$Ni_3Nb(\delta)$ precipitation		$Ni_3Nb(\delta)$, γ', γ'' precipitation
Microfissuring susceptibility	Baseline		Decrease		Increase
Experiment 1	High temperature anneal		Solution anneal $Ni_3Nb(\delta)$		
Experiment 2	High temperature anneal				Age hardening $\gamma' + \gamma''$

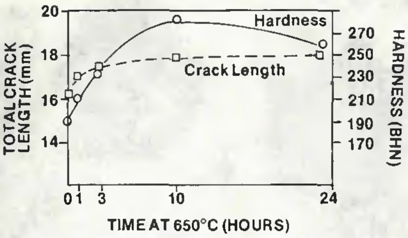

Fig. 9 — A comparison of the change in microfissuring susceptibility with the change in hardness during age hardening. Grain size 60 μm

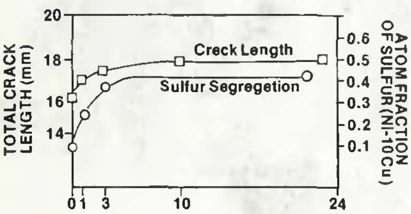

Fig. 10 — Correlation between the change in microfissuring susceptibility and the rate of grain boundary sulfur segregation during age hardening. Grain size 60 μm

ferences and process history. The study was also done in such a way as to eliminate grain size as an unknown variable. Finally, the experimental results indicated that neither $Ni_3Nb(\delta)$ precipitation, nor hardness change, nor $\gamma' + \gamma''$ precipitation were responsible for the observed influence of heat treatment on microfissuring susceptibility. Apparently, the microstructural change which occurs during heat treatment and alters microfissuring susceptibility is a subtle change which our techniques would not be expected to find. One microstructural change which falls in this category is grain boundary segregation of impurities.

Intergranular segregation data for impurities in iron are well established (Ref. 10). It is generally known that impurities concentrate at grain boundaries in a temperature range where both their poor matrix solubility and adequate diffusion rate allow them to move in that direction. The age hardening temperature might be in that range, thus resulting in grain boundary segregation of impurities. It is also known that above a certain temperature the matrix solubility for impurities increases and segregation reverses such that the grain boundary impurity concentration is reduced. Solution annealing could possibly fit in that temperature range.

There is not much intergranular segregation data on nickel alloys, because these alloys are difficult to fracture intergranularly for examination by a technique such as Auger spectroscopy. However, Mulford (Ref. 11) has published sulfur segregation data on a number of binary nickel alloys. The Ni-10Cu alloy of his

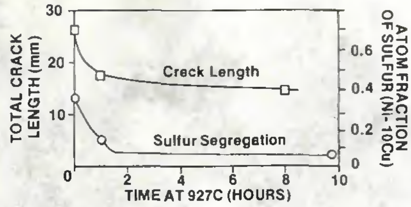

Fig. 11 — Correlation between the change in microfissuring susceptibility and hypothetical sulfur segregation away from grain boundaries during solution annealing. Grain size 200 μm

study is interesting because the kinetics of sulfur grain boundary segregation were given at 650°C (1200°F), which is the same temperature as used in the age hardening treatment of our study. The kinetics of sulfur segregation in Ni-10Cu versus the change in microfissuring susceptibility, both at 650°C, are shown in Fig. 10. The good correlation between sulfur segregation rate and the rate of increase in microfissuring susceptibility is evident. This suggests that microfissuring susceptibility is related to impurity segregation.

Mulford does not present data on the kinetics of segregation at 927°C (1700°F). However, he does state that equilibrium grain boundary segregation is reached in less than one hour above 700°C (1292°F). He also shows that the equilibrium grain boundary sulfur level at 927°C is negligible. Thus, if intergranular sulfur were present prior to solution annealing, it would be removed at a rate similar to the change in microfissuring during solution annealing. This is shown in Fig. 11. It is probable that solution annealing will tend to remove intergranular impurities at a rate similar to the decrease in microfissuring susceptibility.

With many elements and impurities present in sophisticated high-temperature alloys such as 718, it is difficult to say which are involved in intergranular segregation. Certainly, there are many elements involved (Ref. 12) and their combined effect is postulated to control microfissuring in the following manner. Liquid produced by the liquation of some phase, such as Nb(C,N), will either spread over the grain boundary surface or remain at the grain boundary edges or corners. The spreading of this liquid is dictated by the relative surface energies of the grain boundaries and liquid interfaces, as described by Smith (Ref. 13).

Thompson and Genculu (Ref. 6) showed that Nb(C,N) liquation was a prerequisite for microfissuring, regardless of the heat treatment. Solution annealing, which removes impurity from the grain boundary, could promote poor initial grain boundary wetting of the liquating Nb(C,N) and thus reduce microfissuring. A second effect is that impurities would not be present to alter the intergranular liquid chemistry. Thus, the solidification of this liquid over a small temperature range might also be beneficial in reducing microfissuring.

Age hardening, which promotes intergranular segregation, could promote grain boundary wetting of the liquating Nb(C,N) and thus increase microfissuring. The intergranular impurities would also be incorporated into the spreading liquid. This change in liquid chemistry could increase the temperature range during freezing and thus promote microfissuring.

The proposed theory of the effect of impurity segregation on microfissuring still leaves unanswered questions. One obvious question is: Why would solution annealing after an anneal at 1150°C (2130°F) reduce microfissuring? The segregation kinetics of sulfur in Ni-10Cu cannot explain this in terms of a change in intergranular impurity concentration. Classic segregation theory says that, as matrix solubility increases at high temperature, the concentration of elements in the grain boundary should be reduced. Perhaps the change in high temperature phases such as carbides and Laves phases during high temperature annealing accounts for the observed effect. Hopefully, such questions will be answered as research into impurity effects on microfissuring progresses.

Conclusions

The weldability of Alloy 718, with respect to microfissuring susceptibility, is affected beneficially by solution annealing but adversely by age hardening. The magnitude of the weldability change due to heat treatment is dependent on the prior condition of the metal. Large grain size metal, for example, exhibited a larger change in weldability due to heat treatment than small grain size metal.

Phase changes which occurred during heat treatment were not found to correlate with the changes in microfissuring susceptibility. The precipitation of $Ni_3Nb(\delta)$ during solution annealing did not correlate with microfissuring susceptibility. Neither the precipitation of $\gamma' + \gamma''$ nor the change in hardness during age hardening was found to have a direct correlation to changes in microfissuring susceptibility. Since phase changes did not correlate with the observed changes in microfissuring susceptibility, other metallurgical changes were considered.

Metallurgical changes during heat treatment which do not involve phase changes are grain growth, atomic diffusion, and equilibrium atom segregation. The largest grain size metal exhibited the largest change in microfissuring susceptibility during solution annealing but showed no change in grain size. Thus, grain growth during heat treatment was not a significant factor in altering microfissuring. However, the rate of equilibrium grain boundary segregation in binary nickel alloys correlated closely with the changes in microfissuring susceptibility of Alloy 718 during heat treatment. It is postulated that heat treatment alters the intergranular chemistry in such a way that microfissuring susceptibility can either be increased or reduced.

Acknowledgments

The authors wish to thank NASA/Marshall Space Flight Center for supporting this work under NAS8-34962 and Mr. Bob Rowe for his help during the contract. They also thank the National Science Foundation for its support. Acknowledgment also goes to Mrs. Linda Trigg for her work in preparing this manuscript.

References

1. Methods of high-alloy weldability evaluation. 1970. Welding Research Council, Monograph series. New York, N.Y.
2. The Varestraint test. 1982. Welding Research Council. Bulletin 280. New York, N.Y.
3. Thompson, E. G. 1969. Hot cracking studies of Alloy 718 weld heat-affected zone. *Welding Journal* 48(2):70-s to 79-s.
4. Thompson, R. G., Cassimus, J. J., Mayo, D. E., and Dobbs, J. R. 1984. The relationship between grain size and microfissuring in Alloy 718. *Welding Journal* 64(4):91-s to 96-s.
5. Duvall, D. S., and Owczarski, W. A. 1967. Further heat-affected zone studies in heat resistant nickel alloys. *Welding Journal* 46(9):423-s to 432-s.
6. Thompson, R. G., and Genculu, S. 1983. Microstructural evolution in the HAZ of Inconel 718 and correlation with the hot ductility test. *Welding Journal* 62(12):337-s to 345-s.
7. Vincent, E. R. 1980. The microstructure of welds in Inconel 718. Department of Physics, University of Bristol, United Kingdom.
8. Owczarski, W. A., Duvall, D. S., and Sullivan, C. P. 1966. A model for HAZ cracking in nickel-base superalloys. *Welding Journal* 45(4):145-s to 155-s.
9. Savage, W. F., and Krantz, B. M. 1971. Microsegregation in autogenous Hastelloy X welds. *Welding Journal* 50(7):292-s to 303-s.
10. Fundamentals of grain boundary segregation. 1977. Symposium of AIME-TMS. *Metallurgical Transactions* 8A(9):1362-1438.
11. Mulford, R. A. 1983. Grain boundary segregation in nickel and binary nickel alloys doped with sulfur. *Metallurgical Transactions* 14A:865 to 870.
12. Walsh, J. M., and Anderson, N. P. 1976. Characterization of nickel-base superalloy fracture surfaces by Auger electron spectroscopy. *Superalloys*—Proceedings of Seven Springs Conference. AIME-TMS: 127-136.
13. Smith, C. S. 1948. Grains, phases, and interfaces: an interpretation of microstructure. *Transaction A.I.M.M.E.* 175:15-51.